ELSEVIER

Journal of Photochemistry and Photobiology A: Chemistry 148 (2002) 49–55

Journal of Photochemistry and Photobiology A:Chemistry

www.elsevier.com/locate/jphotochem

Contactless determination of the efficiency of photo-induced charge separation in a porphyrin–TiO_2 bilayer

Jessica E. Kroeze*, Tom J. Savenije, John M. Warman

Department of Radiation Chemistry, IRI, Delft University of Technology, Mekelweg 15, 2629 JB Delft, The Netherlands

Received 24 July 2001; received in revised form 6 November 2001; accepted 6 November 2001

Abstract

We have studied photo-induced charge separation in a bilayer consisting of a 60 nm thick layer of a free-base porphyrin spin-coated onto a smooth, 80 nm thick layer of anatase TiO_2 using the (electrodeless) flash-photolysis time-resolved microwave conductivity (FP-TRMC) technique. After correction for direct sub-bandgap excitation, the wavelength dependence of the interfacial incident-photon-to-charge-separation efficiency (IPCSE) closely follows the photon attenuation spectrum of the porphyrin layer from 420 to 700 nm with a maximum value of ca. 0.6% at the Soret band maximum (430 nm). Only the first ca. 1 nm of the porphyrin layer is active in charge separation, i.e. exciton diffusion plays no significant role. Conduction band electrons formed by direct bandgap (300 nm) or sub-bandgap (>400 nm) excitation within the TiO_2 layer decay much more rapidly than those formed by electron injection from the porphyrin layer. In the latter case, the lifetime towards interfacial charge recombination extends well into the millisecond time regime.

Keywords: Porphyrin; Microwave conductivity; Flash-photolysis; Charge separation; TiO_2; Photovoltaics

1. Introduction

Considerable attention has been focussed during the last decades on the possible use of organic antenna molecules for the sensitization of wide-bandgap inorganic semiconductors for applications in photovoltaic devices [1,2]. Since the photoactive region of most of these antenna layers is restricted to a thin layer near the interface with the semiconductor, various ways of overcoming the problems arising from the limited absorption of this photoactive region have been investigated. Substantial increases in conversion efficiencies were obtained with the development of nanocrystalline TiO_2 films, the porous nature of which results in a 1000-fold increase in the surface area accessible to the antenna molecules [3,4]. Other approaches directed towards the improved performance of photovoltaic devices have included the use of interpenetrating conducting polymer networks [5], molecular doping in Schottky-type photovoltaic diodes based on pentacene [6], and increasing the exciton diffusion length within the antenna layer using self-organizing molecules [7].

Central to the overall efficiency of a bilayer photovoltaic device is the wavelength dependence of interfacial charge separation (the "action spectrum"). This parameter is difficult to measure in DC-coupled devices because of the optical and electrical problems associated with the additional electrode layers required for the measurements. We have surmounted these problems by using the flash-photolysis time-resolved microwave conductivity (FP-TRMC) technique to probe the change in conductivity on photoexcitation of inorganic-semiconductor/organic-antenna heterojunctions. In this method, neither electrical contacts nor electrolyte are necessary and the change in conductivity is directly related to the amount of electrons injected into the conduction band of the semiconductor. Recently, the efficiency of charge separation in spin-coated layers of a dialkoxyphenylene-vinylene polymer and a smooth anatase TiO_2 layer was studied quantitatively using this technique [8].

Owing to their strong absorption in the 400–450 nm region (B or Soret band) as well as absorptions in the 500–700 nm region (Q bands), porphyrin derivatives are suitable photosensitizers for the photovoltaic conversion of solar energy. Several photosensitization studies by porphyrins have been reported [4,9–12].

In this work, we present results of a quantitative investigation of photo-induced charge separation in a TiO_2/porphyrin bilayer with a well-defined interface. Free base 5,10,15,20-tetrakis(4-carboxyphenyl)porphyrin, hereafter denoted H_2TPPC (see Fig. 1 for structure), was chosen as a sensitizer, since it is readily processible by spin-coating, and

* Corresponding author. Fax: +31-15-278-7421.
E-mail address: kroeze@iri.tudelft.nl (J.E. Kroeze).

1010-6030/02/$ – see front matter
PII: S1010-6030(02)00038-2

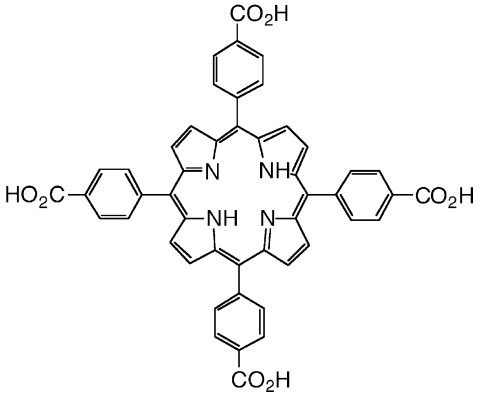

Fig. 1. The molecular structure of 5,10,15,20-tetrakis(4-carboxyphenyl)-porphyrin (H_2TPPC).

its carboxy groups ensure an intimate contact of the macrocycle with the semiconductor surface [12]. A recent study showed that in nanoporous TiO_2 covered with H_2TPPC, electron injection from the excited state of the porphyrin occurs within the picosecond time domain, while recombination takes place on milliseconds [13]. The HOMO and LUMO energy levels of H_2TPPC [14] and the valence and conduction band positions of anatase TiO_2 [15] are shown in Fig. 2, together with the primary and secondary processes that may occur on optical excitation.

In this work, the efficiency of charge separation was determined by relating the conductivity resulting from photoabsorption in the porphyrin layer on visible photoexcitation, to that observed with 300 nm UV light, which directly generates conduction band electrons in the semiconductor by bandgap excitation.

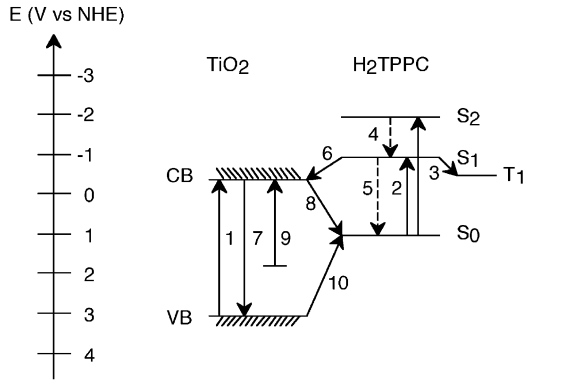

1: direct band gap photoexcitation
2: intramolecular photoexcitation
3: intersystem crossing
4: internal conversion
5: radiationless decay
6: interfacial electron transfer
7: intrinsic charge recombination
8: interfacial charge recombination
9: sub-bandgap excitation
10: interfacial hole transfer

Fig. 2. A schematic diagram of the energy levels of H_2TPPC in solution [14] and the valence and conduction band positions of anatase TiO_2 [15], together with the primary and secondary processes that may occur on optical excitation.

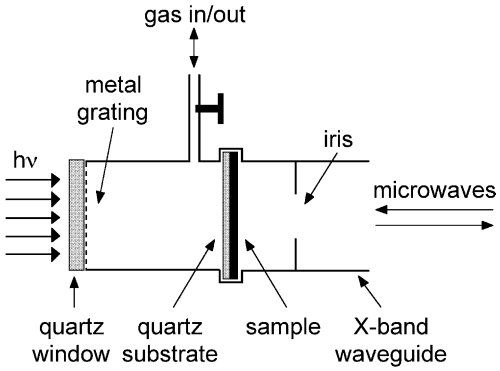

Fig. 3. A schematic representation of the microwave resonant cavity cell used for the electrodeless determination of the change in conductivity occurring on photoexcitation of thin porphyrin and TiO_2 layers.

2. Experimental

Free base 5,10,15,20-tetrakis(4-carboxyphenyl) porphyrin (H_2TPPC) was purchased from Porphyrin Products and used without further purification. A thin film of anatase TiO_2 was deposited on a rectangular ($12 \times 25\,mm^2$), 1 mm thick Suprasil 1 Quartz plate (Heraeus) by Electron Beam Evaporation and subsequently annealed during 24 h at 450 °C, yielding a very smooth and transparent layer, as described previously [15]. H_2TPPC was applied at room temperature on a quartz substrate alone or on the TiO_2 film by spin-coating at 1800 rpm using a 1:1 mixture of pyridine and ethanol as solvent. Immediately after preparation, the sample was mounted in an X-band (8.2–12 GHz) microwave cavity at the position of maximum electric field strength, as shown in Fig. 3, with the TiO_2 layer facing the incident laser beam. After evacuation of the cell to 2×10^{-5} mbar, it was filled to atmospheric pressure with a 10:1 CO_2/SF_6 mixture to suppress any possible signals from highly mobile gas-phase electrons produced by photo-electron emission from the film [16].

The porphyrin layers investigated appeared homogeneous under ×100 magnification. The amount of H_2TPPC adsorbed on the TiO_2 layer was determined by desorption of the dye in 3 ml of ethanol and subsequent measurement of the optical absorption of the solution using a Perkin-Elmer Lambda 40 spectrophotometer. By using the known extinction coefficients of H_2TPPC of 3.4×10^5 (Soret) and 1.6×10^4 (Q_1) [14], it was calculated that 8×10^{-9} moles of the dye were adsorbed per cm^2 of the TiO_2 film. Assuming a density of $1\,g/cm^3$, this corresponds to an H_2TPPC layer thickness of 60 ± 5 nm.

The transmission and reflection spectra of the films were recorded on a Perkin-Elmer Lambda 900 spectrophotometer equipped with an integrating sphere (Labsphere). The optical densities (absorption spectra) of the films were corrected for reflections using

$$\mathrm{OD} = -{}^{10}\log\left(\frac{I_t}{I_0 - I_r}\right) \quad (1)$$

in which I_t is the transmitted, I_0 the incident and I_r the reflected light intensity. The "attenuation spectra", denoting the fraction I_a/I_0 of incident photons actually absorbed by the sample were calculated using

$$\frac{I_a}{I_0} = 1 - \left(\frac{I_t + I_r}{I_0}\right) \quad (2)$$

For photoexcitation with visible light, the third harmonic of a Q-switched Nd:YAG laser (Infinity, Coherent) was used to pump an OPO yielding pulses of ca. 3 ns FWHM continuously tunable from 420 to 700 nm. For wavelengths in the UV, the visible light pulses from the OPO were frequency doubled by an SHG yielding pulses of 2.5 ns FWHM and selected using a Glan-Taylor polarizer. The incident intensity was measured using a Labmaster power meter (Coherent) in combination with a pyroelectric sensor. The beam was directed to the measuring cell using right angle prisms diverged by CaF_2 lenses and attenuated using metal-coated neutral density filters (Melles Griot). The beam cross-section at the position of the cell was rectangular with dimensions close to those of the quartz substrate. The intensity distribution was uniform over the cross-section of the beam and completely free of hot spots. The intensity of every laser pulse was measured by directing the ca. 8% reflection of the laser pulse from a quartz plate into a second, sensitive pyroelectric sensor, from which the intensity ratio to the incident light at the sample position was determined over the full laser wavelength region prior to each experiment.

The change in the microwave power reflected by the cell on illumination was monitored using microwave circuitry and detection equipment which has been fully described previously [17]. To monitor the conductivity change during and shortly after the laser pulse, a Tektronix TDS 680B digitizer was used. Long-lived transients were recorded with a Sony/Tektronix RTD 710A digitizer, which covered the time domain from tens of nanoseconds to milliseconds on a logarithmic time base. By combining the transients obtained with these two digitizers, the complete conductivity formation and decay upon photoexcitation could be monitored from nanoseconds to milliseconds. To improve the signal-to-noise ratio, conductivity transients were averaged over 4–64 single pulses. The overall time response of 18 ns of the set-up was determined mainly by the loaded Q-factor of the resonant cavity.

The change in reflected microwave power ΔP is related to the photo-induced change in conductivity $\Delta\sigma$ of the sample by the sensitivity factor A:

$$\frac{\Delta P}{P} = -A\Delta\sigma \quad (3)$$

Here A was determined to be $3.2 \times 10^{-3}\,\mathrm{mS}^{-1}$ as described previously [18], using the positions, thicknesses and dielectric constants of the media present in the cell.

The conductivity change is related to the sum of the concentration N (m^{-3}) and mobility μ ($\mathrm{m}^2/\mathrm{V\,s}$) of charge carriers present by

$$\Delta\sigma = e\sum N_i\mu_i \quad (4)$$

The data are presented in the form of the parameter $\eta\sum\mu$, which is defined by

$$\eta\sum\mu = \frac{\Delta\sigma\, L}{eI_0} \quad (5)$$

in which I_0 is the incident flux in the pulse (photons/m^2), L the thickness of the layer (m) and η the elementary charge (C). For the formation of a single type of charge carrier pair, η is the yield of pairs present at a given time based on the total number of incident photons and $\sum\mu$ the sum of the mobilities of the positive and negative charge carriers.

3. Results and discussion

3.1. Optical characterization

Fig. 4 shows the separate absorption spectra of a TiO_2/H_2TPPC (80 nm/60 nm) bilayer, a bare 60 nm H_2TPPC layer and a bare 80 nm TiO_2 layer, all on a 1 mm thick quartz substrate. Due to the small overlap of the TiO_2 and the H_2TPPC spectra for wavelengths below 350 nm and above 400 nm, photons of these energies will be almost solely absorbed either in the semiconductor or in the porphyrin, respectively. This allows the selective generation of charge carriers in the TiO_2 conduction band either directly by bandgap excitation using UV light or indirectly by sensitization in the visible. The results obtained in the UV and visible region are discussed separately below.

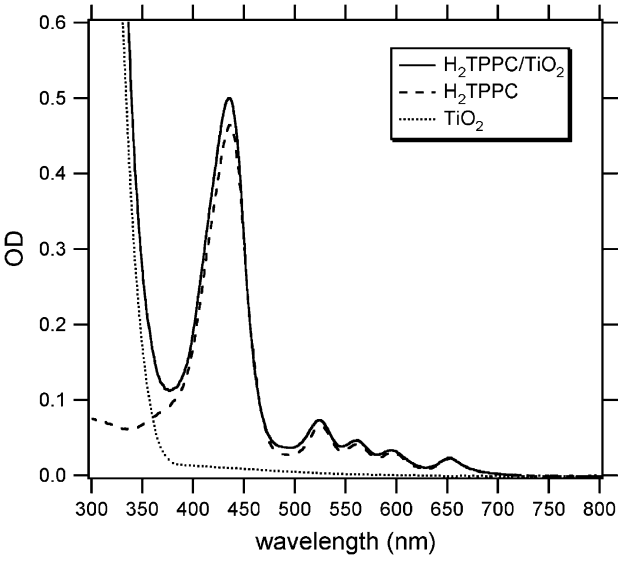

Fig. 4. Absorption spectra (corrected for reflections) of a TiO_2/H_2TPPC bilayer (full line), a 60 nm thick H_2TPPC layer alone (dashed line) and an 80 nm thick bare TiO_2 layer (dotted line).

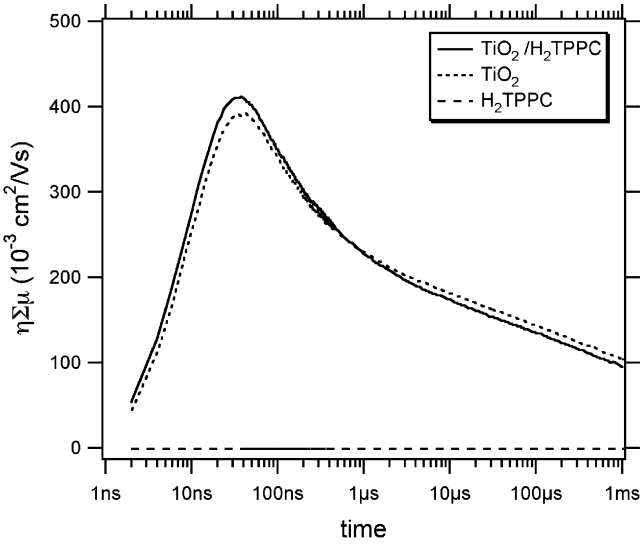

Fig. 5. TRMC transients obtained on photoexcitation at 300 nm of a TiO_2/H_2TPPC bilayer, a bare TiO_2 layer and a bare H_2TPPC layer.

3.2. Photoconductivity transients at 300 nm

Fig. 5 shows the TRMC transients obtained on excitation at 300 nm of a TiO_2/H_2TPPC bilayer, a bare TiO_2 layer and a bare H_2TPPC layer. For the bare porphyrin layer, no measurable photoconductivity was observed. The large signals monitored for both the TiO_2/H_2TPPC bilayer and the bare TiO_2 layer are attributed to the formation of mobile charge carriers in the TiO_2 layer by direct bandgap excitation, as indicated by process 1 in Fig. 2. Taking the charge separation quantum efficiency per absorbed photon to be unity, which is reasonable for anatase TiO_2 [19], together with an observed reflection of 20% at this wavelength, the value of the mobility found is $\sum \mu = 0.5\,cm^2/V\,s$. This value is similar to previously reported values [18,20], and is mainly attributed to the high mobility of electrons in this material, i.e. $\sum \mu \approx \mu_e$.

An important aspect when comparing the 300 nm transients for TiO_2 alone and the TiO_2/H_2TPPC bilayer is that not only are the initial after-pulse heights almost the same, but the decay kinetics are also very similar. We conclude that the process responsible for the conductivity decay in both cases is therefore intrinsic charge carrier trapping and/or charge recombination within the TiO_2 layer.

As is shown in the following section, charge separation across the TiO_2/H_2TPPC interface results in a very much longer lifetime of the photoconductivity. The fact that a much longer lifetime is not observed on direct bandgap excitation of TiO_2 in the TiO_2/H_2TPPC bilayer therefore indicates that hole transfer from TiO_2 to the porphyrin (process 10 in Fig. 2), does not occur, although it should be energetically feasible. However, the large energy difference (exceeding 2 eV) between the TiO_2 valence band and the H_2TPPC HOMO probably causes this hole transfer to take place in the Marcus inverted region.

3.3. Photoconductivity transients between 420 and 700 nm

As was the case for 300 nm flash-photolysis, no measurable conductivity change could be observed on irradiation of the bare H_2TPPC layer for wavelengths in the visible region. Readily measurable photoconductivity transients were, however, found for the TiO_2/H_2TPPC bilayer. The transient monitored on flash-photolysis at 524 nm (the maximum of the Q band) is shown in Fig. 6. Similar transients were observed for other excitation wavelengths in the visible region. In all cases, the transients consisted of a rapidly decaying component in the microsecond time domain followed by a much more slowly decaying component which extended to milliseconds.

In Fig. 7, the magnitudes of the transients at 50 and 500 ns after the pulse are plotted as a function of wavelength. For the shorter time, a relatively structureless spectral dependence is observed whereas at the longer elapsed time features similar to those present in the porphyrin absorption spectrum begin to become apparent. We attribute these observations to the occurrence of two formation pathways for conduction band electrons on photoexcitation of the bilayer: direct formation via sub-bandgap excitation of the TiO_2 (Fig. 6) and interfacial electron injection resulting from photons absorbed in the porphyrin layer. The former process results in the formation of both electrons and holes within the TiO_2 layer and is followed by relatively rapid recombination. The latter process leads to charge separation across the semiconductor/antenna interface and, apparently, results in a much slower decay of the conduction band electrons via interfacial charge recombination with radical cations in the porphyrin layer. Evidence for a very slow rate of interfacial recombination for the TiO_2/H_2TPPC couple has also been found in a time-resolved optical absorption study [13]. In that work, less than half of the separated charges were found to have decayed after a millisecond, in agreement with the present observations. The retardation of interfacial recombination could possibly be due to diffusion of the oppositely charged carriers away from the interface.

In accordance with the above interpretation, photoexcitation of a bare TiO_2 layer in the 420–700 nm region is found to result in conductivity transients which, while much smaller than those observed for direct bandgap excitation at 300 nm, are similar in magnitude to those observed in the visible for the bilayer. Moreover, these sub-bandgap transients decay on the same timescale as the "fast" component found for the bilayer, as shown in Fig. 6.

In order to derive the photoconductivity contribution originating from absorption in the porphyrin layer alone, a "sub-bandgap component" has therefore been subtracted from the bilayer transients. This component is taken to be of the same temporal form as the transient found on photoexcitation of the bare TiO_2 layer at the same wavelength and its relative contribution is weighted with a factor F_{SB}. This weighting factor was adjusted until the initial,

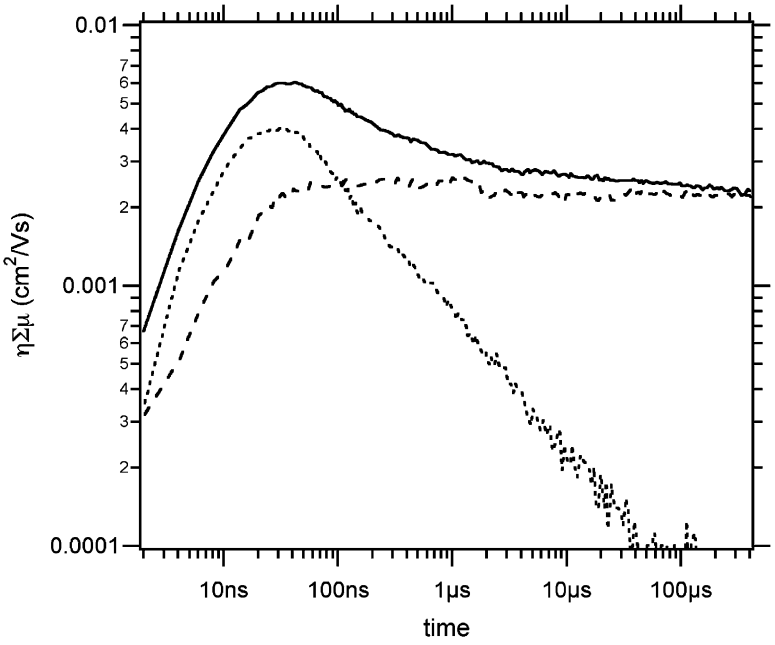

Fig. 6. TRMC transients obtained on flash-photolysis at 524 nm of a TiO_2/H_2TPPC bilayer (solid line), a bare TiO_2 layer weighted by a sub-bandgap correction factor $F_{SB} = 0.9$ (dotted line), and the resulting porphyrin-derived transient $[\eta \sum \mu]_P$ (dashed line).

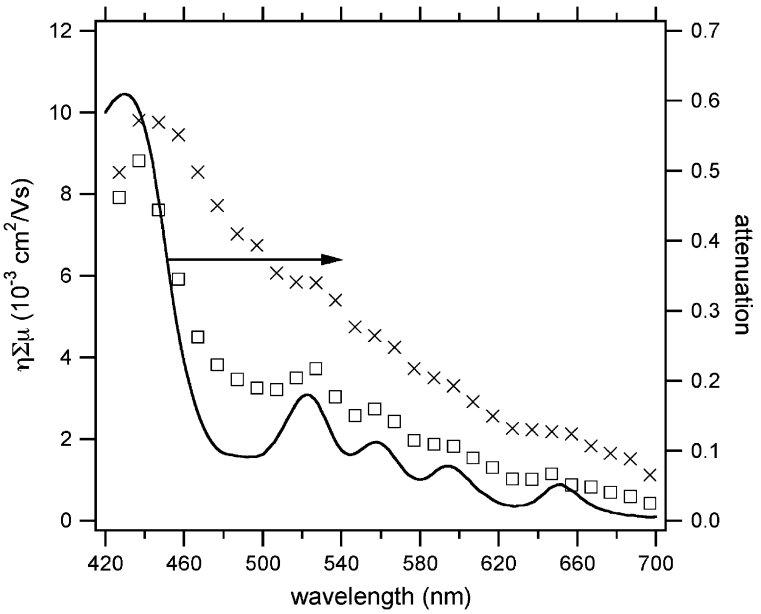

Fig. 7. Wavelength dependence of the magnitude of the TRMC transients at 50 ns (crosses) and 500 ns (squares) after the laser pulse, for a 60 nm thick H_2TPPC layer spin-coated onto a smooth, 80 nm thick layer of anatase TiO_2. The full line represents the fraction of incident photons absorbed by the sample, the 'attenuation' spectrum as given by (2) in the text.

short-timescale decay was compensated. An example of this correction and the resulting porphyrin-derived transient, $[\eta \sum \mu]_P$, is shown in Fig. 6.

The value of $[\eta \sum \mu]_P$ is plotted against wavelength in Fig. 8. The resulting photoconductivity action spectrum is seen to follow closely the spectral dependence of the fraction of photons attenuated in the TiO_2/H_2TPPC bilayer. This agreement indicates that there is no preferential injection of electrons into the TiO_2 layer as a result of excitation in the Soret band. In other words, the rate of internal conversion from S_2 to S_1 would appear to be much more rapid than interfacial electron transfer from S_2. The alternative conclusion that the rates of injection from S_1 and S_2 are identical is considered to be unlikely.

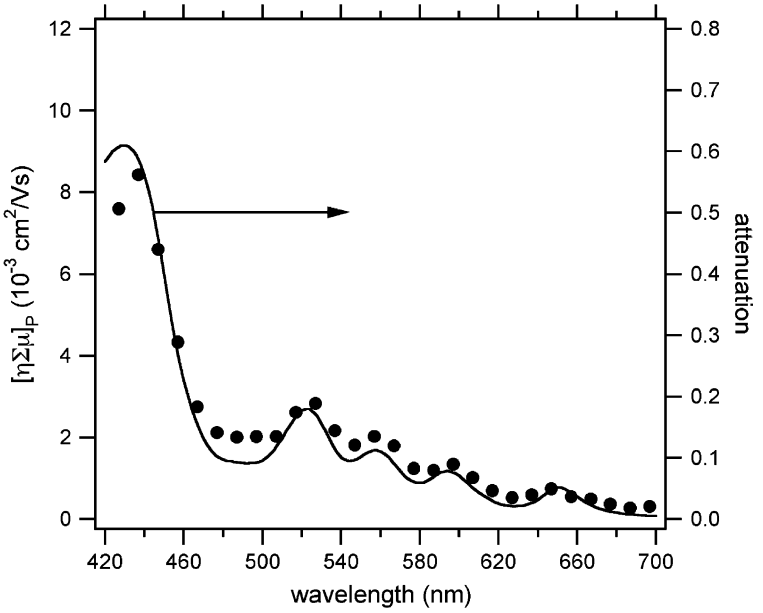

Fig. 8. Wavelength dependence of $[\eta \sum \mu]_P$ for a 60 nm H_2TPPC layer spin-coated onto a smooth, 80 nm thick layer of anatase TiO_2 (filled circles) and the corresponding photon attenuation spectrum.

Intersystem crossing from the lowest excited singlet state to the triplet state, T_1, of metal-free porphyrins is known to occur with high efficiency [14]. As can be seen in Fig. 2, injection of electrons from T_1 into the conduction band of TiO_2 is energetically feasible. However, a recent (sub)picosecond flash-photolysis study on a composite mixture of H_2TPPC and TiO_2 nanoparticles has shown that interfacial electron transfer occurs within 10 ps [13]. Since the timescale for intersystem crossing is several nanoseconds for a metal-free porphyrin, injection via the triplet pathway can be ruled out at least for antenna molecules in the vicinity of the interface.

Intersystem crossing would be expected to occur for excitation in more distant regions of the porphyrin layer. Since the lifetime of the triplet state is many microseconds at least, there is a possibility that triplet excitons could diffuse to the interface from these more distant regions. If injection were to occur via this pathway, however, an after-pulse growth of the conductivity would be expected, which is not the case.

The IPCSE for photons absorbed in the porphyrin layer can be determined from the $[\eta \sum \mu]_P$ value at a given wavelength by comparing this with the value of $\eta \sum \mu$ determined on direct bandgap excitation of TiO_2 at 300 nm, $[\eta \sum \mu]_{300}$, after correction for the fraction of incident 300 nm photons absorbed by the TiO_2 layer, i.e.

$$\text{IPCSE} = \frac{[\eta \sum \mu]_P \, (I_a/I_0)_{300}}{[\eta \sum \mu]_{300}} \times 100\% \qquad (6)$$

In using (6) the underlying assumptions are that the quantum yield for electron–hole pair formation on excitation of anatase TiO_2 at 300 nm is unity and that the mobility of holes is negligible compared with that of electrons.

The maximum value of IPCSE, found at the peak of the Soret band (430 nm), is 0.6%. Since at 430 nm, the fraction of incident photons absorbed by the porphyrin layer in the present sample is 0.6, the quantum yield for interfacial charge separation is only approximately 1%. From this, we conclude that efficient electron injection occurs only from antenna molecules within the first 5–10 Å of the interface, corresponding at most to 2 monolayers. Diffusion of S_1 excitons to the interface from more distant regions of the porphyrin layer would appear to play no role.

In view of the very low efficiency found for the TiO_2/H_2TPPC couple, our current research focusses on increasing the exciton diffusion length within the organic antenna layer. To this end, two possibilities are being investigated: the use of functionalized porphyrin derivatives which form self-organizing columnar liquid crystalline phases, and the use of heavy metal porphyrin derivatives which appear to increase the rate of diffusion of triplet excitons, thus activating the triplet route to sensitization.

4. Conclusions

Photoconductivity transients resulting from flash-photolysis of an inorganic-semiconductor/organic-antenna bilayer heterojunction can be monitored using the time-resolved microwave conductivity technique, without the necessity of applying electrode contact layers. The TRMC photoconductivity action spectrum of a TiO_2/H_2TPPC bilayer corrected for sub-bandgap excitation contributions closely follows the fraction of incident photons absorbed by

the sample, indicating that electron injection into the TiO_2 occurs from the porphyrin first singlet excited state. The maximum quantum yield for interfacial charge separation—appearing at the Soret band (430 nm)—amounts to ca. 1%.

Acknowledgements

The authors thank Roel van de Krol and Barbara van der Zanden (Delft University of Technology) for preparing the EBE TiO_2 samples. The research was supported financially by the Netherlands Organization for Scientific Research (NWO).

References

[1] A. Giraudeau, F.-R.F. Fan, A.J. Bard, J. Am. Chem. Soc. 102 (1980) 5137–5142.
[2] A. Hagfeldt, M. Grätzel, Chem. Rev. 95 (1995) 49–68.
[3] B. O'Regan, M. Grätzel, Nature 353 (1991) 737–740.
[4] A. Kay, M. Grätzel, J. Phys. Chem. 97 (1993) 6272–6277.
[5] J.J.M. Halls, C.A. Walsh, N.C. Greenham, E.A. Marseglia, R.H. Friend, S.C. Moratti, A.B. Holmes, Nature 376 (1995) 498–500.
[6] J.H. Schön, C. Kloc, E. Bucher, B. Batlogg, Nature 403 (2000) 408–410.
[7] B.A. Gregg, J. Sprague, M.W. Peterson, J. Phys. Chem. B 101 (1997) 5362–5369.
[8] T.J. Savenije, M.J.W. Vermeulen, M.P. De Haas, J.M. Warman, Sol. Energy Mater. Sol. Cells 61 (2000) 9–18.
[9] K. Kalyanasundaram, N. Vlachopoulos, V. Krishnan, A. Monnier, M. Grätzel, J. Phys. Chem. 91 (1987) 2342–2347.
[10] G.K. Boschloo, A. Goossens, J. Phys. Chem. 100 (1996) 19489–19494.
[11] H.F. Mao, H.H. Deng, H.W. Li, Y.C. Shen, Z.H. Lu, H.J. Xu, J. Photochem. Photobiol. A 114 (1998) 209–212.
[12] S. Cherian, C.C. Wamser, J. Phys. Chem. B 104 (2000) 3624–3629.
[13] Y. Tachibana, S.A. Haque, I.P. Mercer, J.R. Durrant, D.R. Klug, J. Phys. Chem. B 104 (2000) 1198–1205.
[14] K. Kalyanasundaram, M. Neumann-Spallart, J. Phys. Chem. 86 (1982) 5163–5169.
[15] R. Van de Krol, A. Goossens, J. Schoonman, J. Electrochem. Soc. 145 (1998) 3697.
[16] B.R. Wegewijs, G. Dicker, J. Piris, A.A. Garcia, M.P. De Haas, J.M. Warman, Chem. Phys. Lett. 332 (2000) 79–84.
[17] M.P. De Haas, J.M. Warman, Chem. Phys. 73 (1982) 35–53.
[18] T.J. Savenije, M.P. De Haas, J.M. Warman, Z. Phys. Chem. Int. J. Res. Phys. Chem. Chem. Phys. 212 (1999) 201–206.
[19] A. Shiga, A. Tsujiko, S. Yae, Y. Nakato, Bull. Chem. Soc. Jpn. 71 (1998) 2119–2125.
[20] L. Forro, O. Chauvet, D. Emin, L. Zuppiroli, H. Berger, F. Levy, J. Appl. Phys. 75 (1994) 633–635.